Radiometric and Polarimetric Accuracy Assessment and Calibration of the Hyper-Angular Rainbow Polarimeter (HARP) Instrument

Brent A. McBride[1,2]*, J. Vanderlei Martins[1,2], Roberto Fernandez-Borda[2], Henrique M. J. Barbosa[3]

[1]*Department of Physics, University of Maryland Baltimore County, Maryland, USA*
[2]*Joint Center for Earth Systems Technology, Maryland, USA*
[3]*Instituto de Física, Universidade de São Paulo, São Paulo, Brasil*

**Paper Number: A21B-2158*

**Correspondence to B. McBride at mcbride1@umbc.edu*

Background and Motivation

The Hyper-Angular Rainbow Polarimeter (HARP) is a mission designed to accurately measure microphysical properties of clouds and aerosols from space. A candidate for the NASA Decadal Survey Aerosol-Clouds-Ecosystems (ACE) mission, HARP is a wide field-of-view (FOV), multi-angle imaging polarimeter that splits three spatially-identical images into three independent polarizers and detectors. This technique is the key innovation to achieve high polarimetric accuracy with no moving parts.

The HARP program advances Earth remote sensing in several ways:

- Continues ongoing studies on aerosol-cloud interactions and their climate-related uncertainties [1].
- Sensitivity to non-spherical particles and the variance of a particle or droplet size distribution.
- Angular and spatial resolution improvements over prior and current imaging polarimeters (0.05°, 2.5km spatial)
- Pixel-level retrievals across the entire 114° FOV, avoiding large-scale homogeneity assumptions [2].
- Hyper-angle imaging: 60 unique viewing angles at 0.67um, and 20 at 0.44,0.55, and 0.87um.
- Simultaneous imaging avoids false polarizations [3].
- Highly optimized, refractive optics enables wide FOV measurements in a compact housing and at a fraction of the cost of high-profile satellite missions.
- Global coverage (HARP CubeSat, HARP2) and simple adaptation and integration to a variety of aircraft (AirHARP; B200, ER-2)

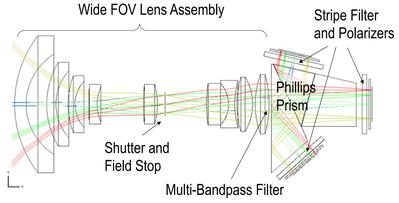

Schematic of the HARP optical assembly.

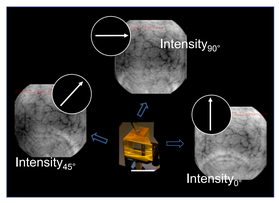

The modified Phillips prism helps separate three unique linear polarization states to three detectors.

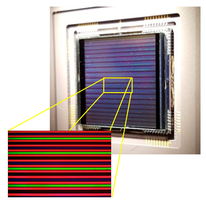

Stripe filters on each detector allow 120 separate viewing angles in 4 HARP passbands.

Imaging Earth at Multiple Viewing Angles

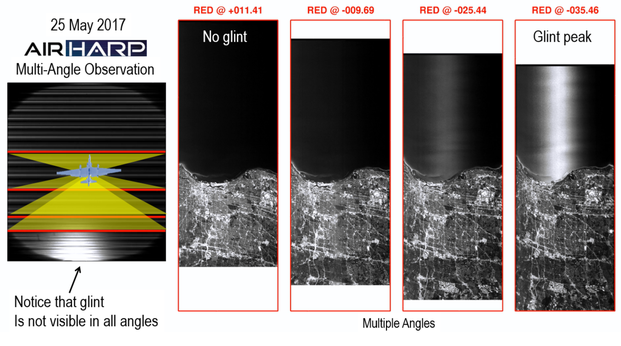

In this example, from the NASA Lake Michigan Ozone Study (05-06/2017), AirHARP observed sunglint over Lake Michigan.

An unprocessed AirHARP image, taken through the detector stripe filter, is shown (far left).

Pushbroom composites (four right images) show the same scene on the ground for different viewing angles, all at 0.67um.

In this way, we can image the angular signature of light scattering from cloud droplets, aerosols, land and ocean surfaces. This information helps to:

- Infer surface and ocean properties (BRDF, pBRDF)
- Retrieve cloud and aerosol microphysics (effective radius, variance, refractive index, cloud thermodynamic phase, AOD, and size distributions)
- Validate assumption-limited retrievals from radiometric satellites (MODIS, VIIRS, ABI, etc.)
- Extend retrievals from vertically-resolved instruments (CALIPSO, CATS, etc.) or other polarimeters (RSP, SPEX, AirMSPI, etc.)

Radiometric and Polarimetric Calibration

For ACE consideration, highly accurate, multi-angular imaging polarimeter instruments are required, especially to retrieve total and polarized information from low light aerosol scenes. This necessitates a rigorous calibration scheme that involves:

- Defining a relationship between detector counts and scene polarization
- Characterizing polarization across the entire HARP FOV
- Verifying the accuracy of the HARP system with models and experiment

Characterizing Polarized and Total Radiances

A rotating polarizer at the aperture of an integrating sphere with known depolarization used to calibrate HARP for polarization.

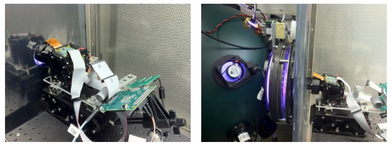

The HARP CubeSat instrument (top left) points into a broadband integrating sphere at UMBC (top right), outfitted with our *polarization dome* at the aperture (below left). Attached to a rotational stage, the dome generates unique and well-controlled angles of completely polarized light.

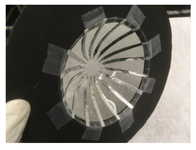

This polarization dome was designed to:

- Maintain ray traces through the HARP front lens
- Retain generated polarization at all points in the FOV

Detector counts (I_j) at a given angle of the polarizer, wavelength, and pixel are related to incident Stokes parameters (I,Q,U) [4]:

$$[\blacksquare I@Q@U\,]1\lambda,px=[\blacksquare C11\ \&C12\ \&C13\ @C21\ \&C22\ \&C23\ @C31\ \&C32\ \&C33\ ]\,[\blacksquare I1\ @I2\ @I3\ ]1\lambda,px$$

Stokes parameters are normalized and defined external to the instrument. The C-matrix that results takes into account all optical interactions inside the system.

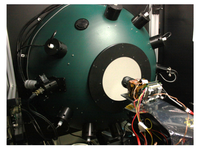

This C-matrix is applied to HARP observations of "Grande", a 1-meter diameter integrating sphere at NASA GSFC Calibration Facility, for radiometry (left).

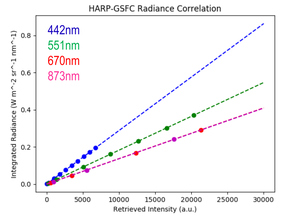

The conversion factor, *k*, between HARP retrieved intensity and integrated spectral radiance of "Grande" is the slope of each line in the comparison figure (right).

For each wavelength, this k-value is then multiplied into the C-matrix so that it converts observed detector counts (a.u.) to scene radiance (W m^{-2} sr^{-1} nm^{-1}):

λ	k *10^{-5}	R^2
442nm	2.8 ± 0.12%	0.99
551nm	1.8 ± 0.10%	0.99
670nm	1.4 ± 0.26%	0.99
873nm	1.4 ± 0.38%	0.99

$$[\blacksquare I@Q@U\,]1\lambda,px=k1\lambda\,[\blacksquare C11\ \&C12\ \&C13\ @C21\ \&C22\ \&C23\ @C31\ \&C32\ \&C33\ ]\,[\blacksquare I1\ @I2\ @I3\ ]1\lambda,px$$

Malus Law and Uncertainties

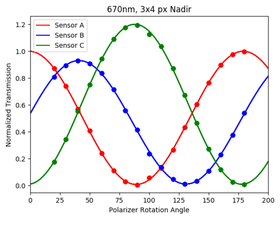

Two polarizer system:

$$I \propto \cos^2\theta$$

Sensor	σ_{RMS} (%)
A (1)	0.450
B (2)	0.587
C (3)	0.714

The Malus' Law [5] intensity profile results, when the HARP instrument observes an integrating sphere through a rotating polarizer. Phase shifts between detectors are relative to the angle of the polarizer in front of each detector.

The system C-matrix and associated error is calculated using a least squares approach, involving measurements of the polarization dome at least three unique rotation angles.

The absolute errors in each Stokes parameter can be derive via:

$$\sigma 1[\blacksquare I@Q@U\,]=\sqrt{\sum_{i=1}^{3}(C1[\blacksquare 1@2@3\,]i\,k1\lambda\ \sigma 1I i\,)^2+(I1i\,k1\lambda\ \sigma 1C1[\blacksquare 1@2@3\,]i\,)^2}+(C1[\blacksquare 1@2@3\,]i\,k1\lambda\ \sigma 1I2\,)^2$$

where the position of the values in brackets correspond to the position of the Stokes parameter in the sigma subscript. The above error terms correspond to the HARP measurement, C-matrix element, and radiometric conversion factor.

Preliminary Accuracy Assessment

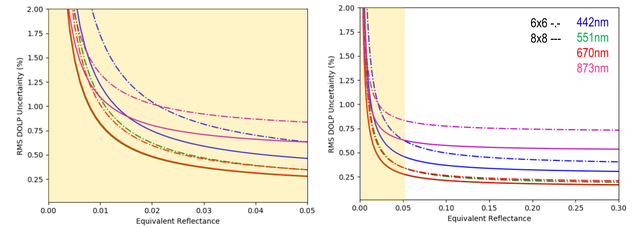

Preliminary modeled $DOLP_{RMS}$ accuracy level of the AirHARP instrument for various binning regimes and wavelengths. Experimental SNR from GSFC radiometric calibration drives a simulated HARP calibration model for the nadir portion of the sensor. This assessment is still in early stages of development.

The HARP2 instrument on-board the PACE payload will see advancements that greatly improve polarimetric accuracy (table, right).

Instrument	Improvements over AirHARP	Impact on SNR
HARP CubeSat	Prism/detector optimization	*
HARP2 (PACE)	Prism/detector optimization	*
	Faster frame speed (>2 f/s)	+2.5-5x
	Enhanced flatfield characterization	*

*Requires sensitivity analysis

Preliminary Cloud Retrieval

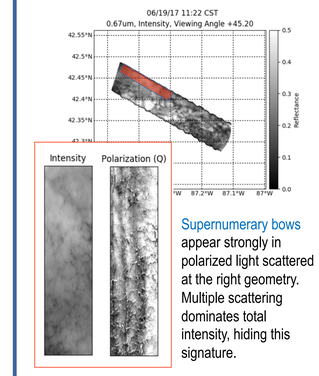

Supernumerary bows appear strongly in polarized light scattered at the right geometry. Multiple scattering dominates total intensity, hiding this signature.

Correcting for viewing and solar geometry following [2], polarized reflectance (R_p) analyzed for an 8x8 pixel region along the principal plane is shown below:

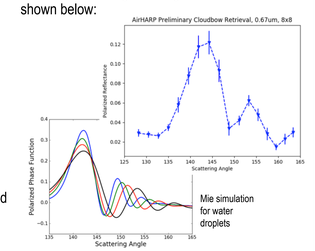

Methods comparing Mie P_{12} (above) to R_p are used to glean the *effective radius* (r_e), *variance* (v_e), and *thermodynamic phase* of a cloud scene.

Future Work

- Application of polarization dome analysis for polarization calibration across the entire FOV
- Continuing L1 and L2 data production and development from LMOS and ACEPOL campaigns
- Intercompare L1 ACEPOL products with RSP, SPEX, AirMSPI for test cases (glint, dark ocean, etc.)
- Assess the viability of GRASP algorithm [6] for multi-pixel aerosol retrieval

References

[1] IPCC, Climate Change 2014: Synthesis Report, Geneva, Switzerland (2014), 151 pp.
[2] F. M. Breon and M. Boucher, IEEE, **43** (2005), pp. 1796-1805.
[3] A. Kohkanovsky and G. de Leeuw, *Sat. Aero. Rem. Sens. Over Land.* Praxis Publishing (2009), p. 298
[4] R. F. Borda et al., SPIE, **7461** (2009), pp. 1-13.
[5] E. Hecht, *Optics*, Addison-Wesley, Reading, MA, (1979).
[6] O. Dubovik et al., AMT, **4** (2011) , pp. 975-1018

This work is funded in part by the NASA Earth and Space Science Fellowship (NESSF) 16-EARTH16F-0243, with renewal extensions through 2019.